A Generative Model for Time and Frequency Domain Parameters

Two Sides from the Same Coin?

Matías Castillo-Aguilar

Introduction

Heart rate variability (HRV), quantified through the analysis of human heart period fluctuations, represents a pivotal noninvasive index of autonomic nervous system (ANS) function. Its utility spans diverse domains, from clinical cardiology to psychophysiology. Methodological advancements in HRV assessment have progressed significantly, evolving from fundamental time-domain descriptors, such as the standard deviation of normal-to-normal intervals (SDNN) and the root mean square of successive differences (RMSSD), to incorporate sophisticated frequency-domain analyses, nonlinear dynamics, and machine learning algorithms. Despite these developments, current approaches confront two persistent and interrelated limitations: a fundamental compromise between temporal precision and frequency resolution in conventional spectral techniques, and the predominantly descriptive or retrospective nature of derived metrics, which often obscure direct insight into underlying physiological mechanisms.

The inherent time-frequency compromise in classical spectral analysis critically impedes the accurate characterization of autonomic events occurring over brief timescales. Employing extended analysis windows to achieve fine spectral discrimination risks temporal blurring or complete obscuration of rapid sympathetic or parasympathetic modulations. Conversely, shortening the analysis window to capture transient phenomena necessarily diminishes the precision with which distinct frequency components can be resolved. This analytical dilemma holds substantial clinical relevance. For instance, the detection of abrupt vagal withdrawal during orthostatic challenge, sympathetic surges in response to acute stressors, or stage-dependent autonomic shifts during sleep is often critical for diagnosis and intervention. The absence of a robust, principled framework to circumvent this trade-off consequently constrains both research and clinical application.

Furthermore, the interpretive discontinuity between descriptive spectral estimates and their physiological causation diminishes the explanatory power of HRV metrics. Standard analytical practice frequently reduces dynamic spectral

information into aggregated indices, such as the low- to high-frequency (LF/HF) power ratio or band-specific power in normalized units. While serving as proxies for sympathetic and parasympathetic balance, these scalar summaries obscure whether observed alterations in spectral ratios result from genuine increases in one component, decreases in another, or simultaneous modulations of both. This ambiguity complicates mechanistic inference, inter-study comparability, and translation to therapeutic interventions.

Prior attempts to address these limitations, including the application of nonlinear measures (e.g., entropy, fractal dimension) or data-driven decompositions (e.g., empirical mode decomposition, supervised learning classifiers), offer valuable complementary perspectives. However, these methods frequently sacrifice physiological transparency for mathematical or predictive sophistication. Nonlinear indices quantify signal complexity without directly mapping to specific autonomic pathways. Data-driven modes necessitate post-hoc labeling to associate extracted components with vagal or sympathetic processes. Machine learning models, while effective in classification tasks, typically function as opaque "black boxes" devoid of mechanistic interpretability. Therefore, a compelling need persists for an analytical paradigm that unifies temporal and spectral characterization within a generative, physiologically grounded framework.

In response to these challenges, we propose a novel parametric model of the R–R interval (RRI) signal. This model concurrently captures: (i) slow, trending variations in the baseline heart period; (ii) dynamic changes in the overall amplitude of rhythmic variability; and (iii) instantaneous allocation of spectral power across the very-low (VLF), low (LF), and high (HF) frequency bands. Central to this formulation is the representation of each latent component as an explicit, time-varying function, parameterized by physiologically interpretable constructs. Baseline trends are accommodated by smooth parametric functions that model circadian drift and tonic autonomic shifts. The total amplitude of structured variability is represented by a separate time-varying scale parameter, analogous to a dynamic SDNN, thereby isolating global autonomic drive from spectral composition. Spectral proportions are subsequently derived through a hierarchical stick-breaking decomposition: a double-logistic function specifies the fractional contribution of VLF power, and a second double-logistic function governs the HF-to-LF ratio within the residual non-VLF portion. This two-stage stick-breaking approach reduces latent dimensionality, preserves natural physiological ordering, and endows each parameter with direct mechanistic significance, encompassing rise and fall kinetics, baseline levels, and recovery dynamics.

By integrating these parametric latent processes within a single generative equation, the proposed model transcends the retrospective nature of conventional spectral analysis. It yields instantaneous estimates of band-specific power without recourse to sliding windows or arbitrary smoothing, thereby obviating the time-frequency trade-off. Concomitantly, it retains the capacity to simulate synthetic RRI trajectories under controlled autonomic scenarios, enabling rigorous

power analyses, hypothesis testing, and educational demonstrations. Critically, parameter estimates derived from empirical data possess immediate physiological interpretability: they map directly to the timing, magnitude, and duration of sympathetic activation and parasympathetic recovery events.

The implications of this unified generative paradigm are substantial. In basic research, it facilitates mechanistic investigations into autonomic regulation, permitting the quantitative assessment of coupling between respiratory patterns and heart rate, or the precise delineation of recovery kinetics following physical exertion. Clinically, it offers refined biomarkers for dysautonomia, heart failure, and stress-related disorders, enhancing both diagnostic sensitivity and prognostic specificity. Within wearable technology and biofeedback applications, it supports real-time monitoring of autonomic state, guiding adaptive interventions tailored to instantaneous physiological need.

In summary, we present a formalized, physiologically coherent generative model of heart rate variability that reconciles temporal and spectral analysis within a single, interpretable framework. By embedding parametric latent drives for baseline heart period, variability amplitude, and spectral composition, the model offers enhanced resolution, transparency, and applicability across multidisciplinary contexts. This approach is anticipated to serve as a foundational advance in HRV research, catalyzing a transition from descriptive heuristics to a quantitatively precise science of autonomic cardiovascular dynamics.

Model formulation

We consider a discrete set of time points $\{t_i\}_{i=1}^{N}$ at which the R–R interval (RRI) signal is observed. The objective is to represent the RRI series as a superposition of a smoothly varying baseline component, a time-dependent amplitude of structured variability, and a convex combination of spectral oscillators at physiologically defined frequency bands. This model is formally defined in Equation 1.

$$\mathrm{RRI}(t_i) = \underbrace{\mathrm{RR}(t_i)}_{\substack{\text{baseline heart period}}} + \underbrace{\mathrm{SDNN}(t_i)}_{\substack{\text{total modulation}\\ \text{amplitude}}} \times \underbrace{\sum_{j=1}^{3} p_j(t_i)\,\sin(2\pi f_j t_i + \phi_j)}_{\substack{\text{spectral oscillators}\\ \text{weighted by proportions}}} + \varepsilon_i \tag{1}$$

Here, $j = 1, 2, 3$ index the very-low-frequency (VLF), low-frequency (LF), and high-frequency (HF) bands, respectively. The parameters f_j denote the central frequencies, and ϕ_j represent constant phase offsets. Residual, unstructured variability is captured by $\varepsilon_i \sim \mathcal{N}(0, \sigma^2)$. The explicit time dependency of the functions $\mathrm{RR}(t)$, $\mathrm{SDNN}(t)$, and $\{p_j(t)\}$ obviates the need for opaque sliding-window decompositions, thus facilitating the simultaneous modeling of both time-domain and frequency-domain phenomena.

Baseline heart period: $\mathrm{RR}(t)$

The $\mathrm{RR}(t)$ component quantifies the slow, underlying variations in the mean R–R interval. These fluctuations arise from long-term physiological regulatory processes, including circadian rhythms and shifts in tonic autonomic drive. This component can be parameterized effectively using smooth, low-dimensional functions that yield interpretable "onset" and "recovery" parameters. A double-logistic function, as presented in Equation 2, is particularly well-suited for this purpose.

$$\mathrm{RR}(t) = \underbrace{\alpha}_{\substack{\text{Baseline} \\ \text{level}}} - \underbrace{\frac{\beta}{1 + e^{-\lambda\,(t-\tau)}}}_{\substack{\text{Exercise-induced} \\ \text{drop}}} + \underbrace{\frac{c\,\beta}{1 + e^{-\phi\,(t-\tau-\delta)}}}_{\substack{\text{Exercise recovery} \\ \text{kinetics}}} \tag{2}$$

In this formulation, α represents the baseline heart period, which can be interpreted as the tonic vagal level. The parameter β signifies the magnitude of the exercise-induced decline in RR. The rate constant λ governs the initial decrease, with its inflection point occurring at time τ. The fractional recovery amplitude is denoted by c, while ϕ represents the recovery rate. Finally, δ quantifies the temporal offset between the decline and recovery phases.

This specific formulation, previously validated by Castillo-Aguilar et al. (2025), directly estimates physiologically salient time points and magnitudes. This facilitates enhanced mechanistic interpretation and improved comparability across different studies.

Structured variability amplitude: $\mathrm{SDNN}(t)$

In the proposed model, $\mathrm{SDNN}(t)$ functions as a time-varying scale parameter that quantifies the instantaneous magnitude of oscillatory variability, thereby generalizing the conventional standard deviation of NN intervals. By decoupling $\mathrm{SDNN}(t)$ from spectral composition, the model effectively isolates global autonomic modulation strength from relative band contributions. Analogous to $\mathrm{RR}(t)$, $\mathrm{SDNN}(t)$ can be represented by a double-logistic function, consistent with the form outlined in Equation 2. This approach permits an identical interpretation of function parameters across both the $\mathrm{RR}(t)$ and $\mathrm{SDNN}(t)$ components.

A significant advantage of employing the same functional form for both time-domain components is the ability to specify shared parameters between mean RRI and SDNN. This facilitates the derivation of more biologically meaningful parameters related to autonomic modulation capacity.

Spectral composition via Stick-Breaking

The instantaneous proportions of the total oscillatory amplitude attributed to each frequency band are denoted by $p_{\mathrm{VLF}}(t)$, $p_{\mathrm{LF}}(t)$, and $p_{\mathrm{HF}}(t)$. To enforce the

constraints $0 \leq p_j(t) \leq 1$ and $\sum_j p_j(t) = 1$ with minimal latent dimensionality, a two-stage stick-breaking scheme is employed. This method systematically allocates proportions, ensuring they sum to unity while remaining within valid ranges.

First, the functional form for the VLF proportion, p_{VLF}, is defined in Equation 3.

$$p_{\text{VLF}}(t) = \alpha_{\text{VLF}} + \frac{\beta_{\text{VLF}}}{1 + e^{-\lambda_{\text{VLF}}(t-\tau_{\text{VLF}})}} - \frac{c_{\text{VLF}}\,\beta_{\text{VLF}}}{1 + e^{-\phi_{\text{VLF}}(t-\tau_{\text{VLF}}-\delta_{\text{VLF}})}} \tag{3}$$

This represents a double-logistic function, a flexible yet parsimonious mathematical form, characterized by physiologically interpretable parameters: α_{VLF}, β_{VLF}, c_{VLF}, λ_{VLF}, ϕ_{VLF}, τ_{VLF}, and δ_{VLF}. These parameters allow the model to capture the dynamic "onset" and "recovery" phases of VLF contribution, reflecting physiological changes over time.

Next, the HF fraction of the non-VLF remainder, which comprises both HF and LF proportions, is estimated. This proportion, representing the relative balance between HF and LF activity within the non-VLF portion, is defined in Equation 4.

$$r_{\text{HF/LF}}(t) = \frac{p_{\text{HF}}(t)}{p_{\text{HF}}(t) + p_{\text{LF}}(t)} \tag{4}$$

This ratio is further modeled as proposed in Equation 5, also employing a double-logistic function to capture its temporal dynamics.

$$r_{\text{HF/LF}}(t) = \alpha_r + \frac{\beta_r}{1 + e^{-\lambda_r(t-\tau_r)}} - \frac{c_r\,\beta_r}{1 + e^{-\phi_r(t-\tau_r-\delta_r)}} \tag{5}$$

Subsequently, the individual proportions for HF and LF are computed using the previously defined $p_{\text{VLF}}(t)$ and $r_{\text{HF/LF}}(t)$ to ensure the sum-to-one constraint. This procedure, derived from the stick-breaking logic, is formally presented in Equation 6.

$$\begin{aligned} p_{\text{HF}}(t) &= [1 - p_{\text{VLF}}(t)]\, r_{\text{HF/LF}}(t) \\ p_{\text{LF}}(t) &= [1 - p_{\text{VLF}}(t)][1 - r_{\text{HF/LF}}(t)] \end{aligned} \tag{6}$$

This calculation is justified because the term $[1 - p_{\text{VLF}}(t)]$ inherently represents the combined proportion of $p_{\text{HF}}(t) + p_{\text{LF}}(t)$. Therefore, multiplying this remainder by $r_{\text{HF/LF}}(t)$ (which is $p_{\text{HF}}(t)/[p_{\text{HF}}(t) + p_{\text{LF}}(t)]$) directly yields $p_{\text{HF}}(t)$, as the sum of HF and LF proportions cancels out. Similarly, the complement of $r_{\text{HF/LF}}(t)$, denoted as $[1 - r_{\text{HF/LF}}(t)]$, precisely represents the ratio of LF contribution to the non-VLF remainder. Multiplying this by $[1 - p_{\text{VLF}}(t)]$ then correctly computes $p_{\text{LF}}(t)$. This ensures that $p_{\text{HF}}(t) + p_{\text{LF}}(t) + p_{\text{VLF}}(t) = 1$. This construction ensures that $\sum_j p_j(t) = 1$ for all t while preserving a natural

physiological hierarchy, reflecting how a total resource (the full amplitude of variability) is sequentially broken down and distributed among components.

Reparameterization of β and α

The parameters β_{VLF} and β_r, which govern the magnitude of temporal fluctuations in p_{VLF} and $r_{\text{HF/LF}}$, are not inherently constrained to the $[0, 1]$ interval. This lack of constraint can pose challenges for gradient-based samplers, as their efficiency relies on navigating the posterior geometry effectively. While defining narrow priors could partially mitigate this issue, such a strategy presupposes substantial prior knowledge regarding the temporal dynamics of the relative contributions for each spectral component. Given the novelty of these generative models in the continuous modeling of spectral HRV components, such an assumption is, at best, speculative.

A more robust approach involves transforming the parameters that control these dynamics to ensure the system's behavior remains within physiologically plausible ranges. In this context, an inverse logit transformation effectively constrains the output scale while permitting an unconstrained parameter space, as defined in Equation 7.

$$\beta = \frac{e^{\beta_{\mathbb{R}}}}{1 + e^{\beta_{\mathbb{R}}}} - \alpha \tag{7}$$

Here, the new parameter $\beta_{\mathbb{R}}$ represents the unconstrained transformation of β, where $\beta_{\mathbb{R}} \in \mathbb{R}$. The term α denotes the baseline level in the proportion of p_{VLF} and $r_{\text{HF/LF}}$.

Furthermore, the α parameter can undergo a similar transformation to be constrained within the same range, thereby exhibiting properties analogous to $\beta_{\mathbb{R}}$, as presented in Equation 8.

$$\alpha = \frac{e^{\alpha_{\mathbb{R}}}}{1 + e^{\alpha_{\mathbb{R}}}} \tag{8}$$

Synthesis and interpretability

The integrated model, formally defined by Equation 1 and its associated parameterizations (Equations 2–6), establishes a comprehensive generative framework for analyzing R–R interval dynamics. This framework explicitly represents baseline trends, global modulation strength, and spectral composition as distinct, time-varying latent constructs. This approach provides an unparalleled level of detail in capturing the complex interplay of physiological processes influencing heart rate variability.

The utilization of double-logistic functions for modeling the temporal dynamics of both baseline heart period ($\text{RR}(t)$) and structured variability amplitude ($\text{SDNN}(t)$) is a key feature of this model. These functions offer a parsimonious

yet flexible representation of the physiological onset and recovery kinetics, which are fundamental to understanding dynamic physiological responses. This mathematical formulation enables the direct estimation of physiologically meaningful indices, such as the precise timing of a physiological surge onset, the magnitude of peak amplitudes, and the duration of half-recovery phases. These derived parameters are not merely statistical artifacts; they offer direct, interpretable insights into underlying biological mechanisms.

Furthermore, the implementation of a stick-breaking decomposition for spectral composition significantly reduces the latent dimensionality of the model. This ensures that the estimated spectral proportions are both inherently interpretable and mathematically constrained to a simplex, reflecting their nature as fractional contributions. This rigorous parametric framework fundamentally obviates the need for ad hoc sliding windows and arbitrary smoothing techniques, which often introduce latency and distortion into the analysis of time-varying physiological signals. Consequently, the model delivers precise, transparent, and mechanistically grounded insights into the intricate processes governing autonomic cardiovascular regulation, representing a substantial advancement in the field.

Simulating R-R interval data

To demonstrate the practical application of the proposed generative framework, we will simulate an R-R interval time series under controlled, physiologically plausible conditions. This process begins by establishing constant baseline proportions for the three canonical frequency bands: high-frequency (HF), low-frequency (LF), and very-low-frequency (VLF). Subsequently, we introduce temporal dynamics into both the mean R-R interval and its variability envelope.

Initially, we establish equal contributions from each frequency band, setting each proportion to one-third. This represents a neutral starting point, ensuring no single band is presumed to dominate the overall spectral composition:

$$
\begin{aligned}
p_{\mathrm{HF}} &\leftarrow 0.\overline{333} \\
p_{\mathrm{LF}} &\leftarrow 0.\overline{333} \\
p_{\mathrm{VLF}} &\leftarrow 0.\overline{333}
\end{aligned}
$$

These assignments for p_{HF}, p_{LF}, and p_{VLF} represent the constant fractional weights of the HF, LF, and VLF components, respectively. This uniform initialization provides a balanced baseline from which subsequent temporal modulations will evolve, facilitating clear attribution of dynamic changes to the logistic-driven processes described later.

Next, we assign central frequencies f_j for each sinusoidal oscillator based on established heart rate variability (HRV) spectral ranges. Selecting values at

the midpoint of each band ensures that our simulated oscillations reside within physiologically validated domains:

Band	Frequency range (Hz)
HF	0.15–0.40
LF	0.04–0.15
VLF	0.003–0.04

The approximated frequency for each band is set to the midpoint of its range: $f_{\mathrm{HF}} \approx 0.25$, $f_{\mathrm{LF}} \approx 0.10$, and $f_{\mathrm{VLF}} \approx 0.02$. For the random phase parameter ϕ_j, we will draw them from $\phi_j \sim \mathcal{U}(0, 2\pi)$. This assumption of out-phase oscillations at simulation onset allows for more realism of the resultant beat-to-beat variability.

Subsequently, temporal modulation of both the mean R-R interval and its standard deviation (SDNN) is incorporated using coupled double-logistic functions, consistent with the parameterization described by Castillo-Aguilar et al. (2025). The parameters governing the mean R-R trajectory are defined as follows:

Parameter	Value	Meaning
α_{RR}	800	Baseline RR
β_{RR}	300	RR drop
c_{RR}	0.80	Recovery proportion
λ_{RR}	3.0	Drop rate
ϕ_{RR}	2.0	Recovery rate
τ_{RR}	6.0	Drop time
δ_{RR}	3.0	Drop duration

These parameters establish a baseline R-R interval of 800 ms, a transient decrease of 300 ms upon exercise onset, and an 80% recovery over a subsequent window, with precisely defined rates and timing.

An analogous parameter set governs the time course of SDNN:

Parameter	Value	Meaning
α_{SDNN}	48	Baseline SDNN
β_{SDNN}	32	SDNN drop
c_{SDNN}	1.20	Recovery proportion
λ_{SDNN}	2.0	Drop rate
ϕ_{SDNN}	2.0	Recovery rate
τ_{SDNN}	6.0	Drop time
δ_{SDNN}	3.0	Drop duration

Here, resting variability commences at 48 ms, transiently decreases by 32 ms with exercise, and subsequently overshoots the baseline by 20% during the recovery phase, thereby reflecting dynamic autonomic modulation.

A high-resolution time vector is defined, spanning from 0.01 min to 15 min in 0.01 min increments, ensuring fine temporal granularity for the simulation. Using these specifications, the mean R-R interval at each time point is computed via the double-logistic form previously described. This generates a time series that smoothly transitions from baseline to nadir and back toward recovery, effectively capturing the characteristic heart period modulation induced by exercise. The same generative process is applied to SDNN fluctuations over time, utilizing an identical functional form as for the mean R-R interval. This dynamic relationship is depicted in Figure 1.

The SDNN(t) curve represents the width around the main R-R interval signal. This can be re-visualized as a band of varying width around the mean R-R interval signal, as depicted in Figure 2.

The amplitude of this band, determined by SDNN(t), demonstrably changes over time. This variation is directly linked to autonomic modulation, underscoring its inherently dynamic nature. It is crucial to recognize that the width of this amplitude band serves as the container for fluctuations originating from the frequency domains.

Integration of frequency-domain components

Frequency domains, which constitute the segment of the R-R interval signal composed of periodic waves at different frequencies, are the elemental constituents of the signal's amplitude. Consequently, the overall amplitude is formed by the HF, LF, and VLF components, not necessarily in equal proportions. A fundamental assumption prevalent in most spectral decomposition analyses is that the proportional contribution of different frequency bands remains constant over time. This implies that the proportion of the amplitude band described by HF, LF, or VLF does not fluctuate temporally. However, this premise is fundamentally flawed because the autonomic nervous system is a known dynamic system, rendering assumptions of static states physiologically unsound.

This dynamic process is further depicted by the Equation 9, with the fundamental condition $\sum_{j=1}^{J} p_j(t_i)\sin(2\pi f_j t_i + \phi_j) = 1$ to be constrained within the limits of SDNN(t).

$$\sum_{j=1}^{3} \underbrace{p_j(t_i)}_{\substack{\text{Time-evolving} \\ \text{proportion}}} \underbrace{\sin(2\pi f_j t_i + \phi_j)}_{\text{Wave function}} \tag{9}$$

A reference figure illustrating isolated frequency components as a function of time portrayed in Figure 3.

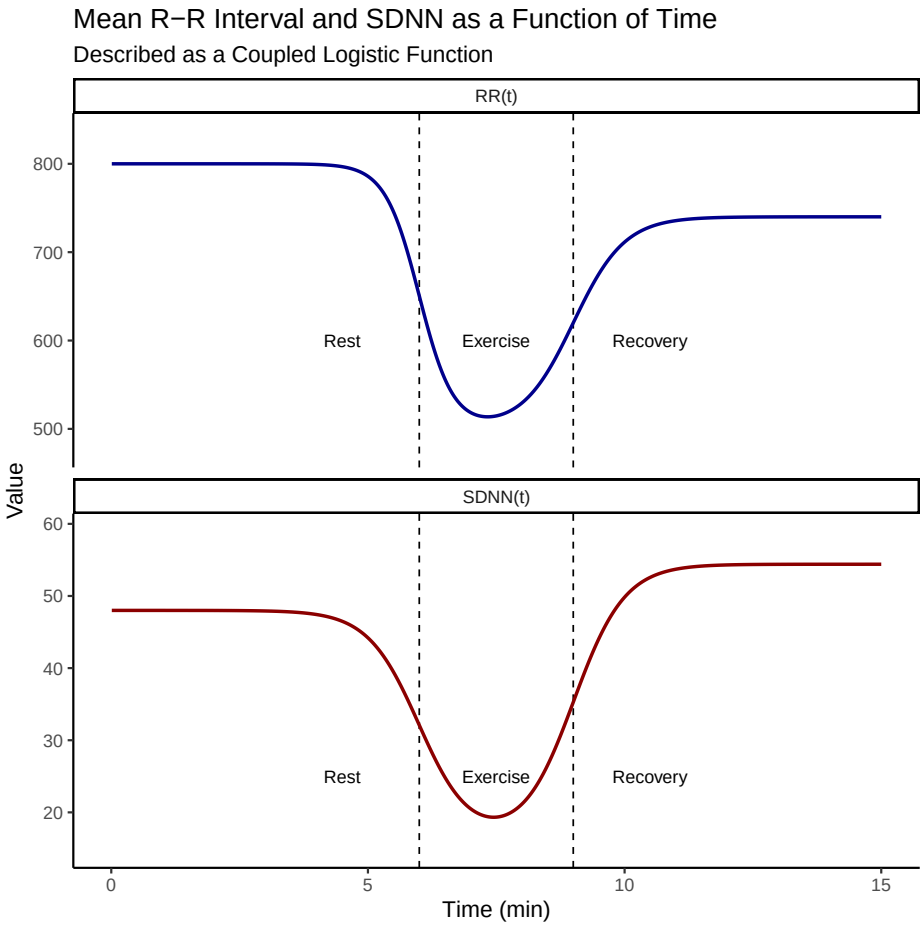

Figure 1: Mean R-R ($\mathrm{RR}(t)$) and SDNN ($\mathrm{SDNN}(t)$) as a function of time, illustrating a resting state, exercise-induced drop, and post-exercise recovery kinetics. This behavior is controlled by the coupled logistic function described.

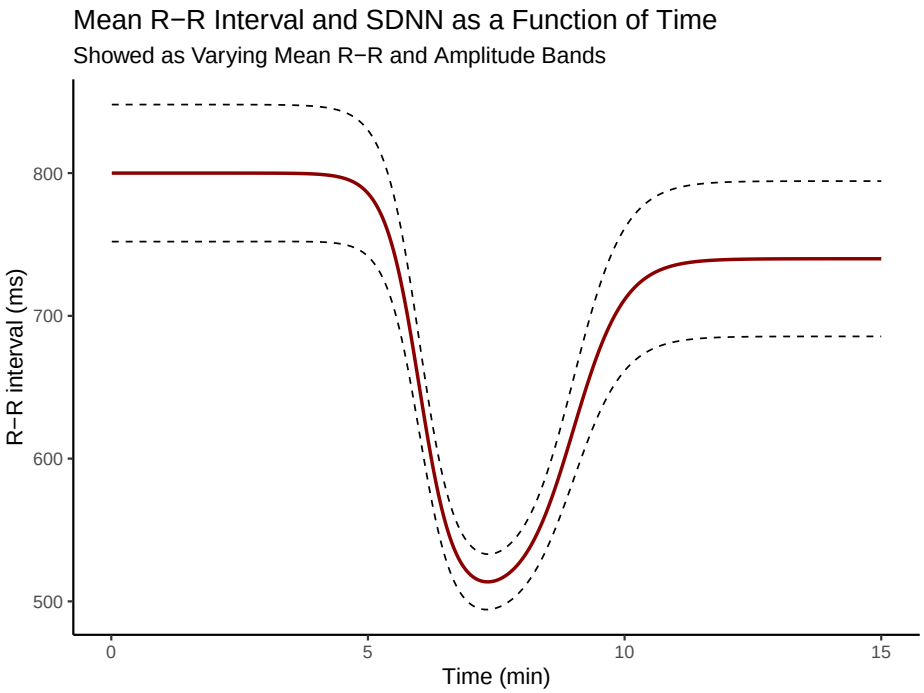

Figure 2: Mean R-R and SDNN as a function of time, where SDNN is depicted as a varying amplitude band around mean R-R, representing fluctuations in HRV.

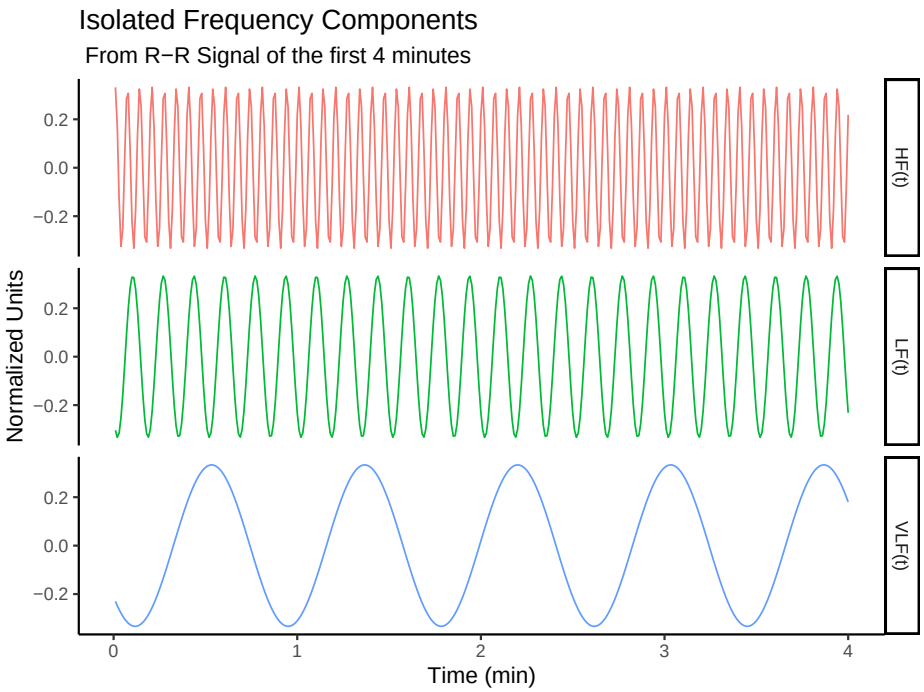

Figure 3: Isolated high, low, and very low frequency components as a function of time during the first 4 minutes. Each frequency band is normalized by its relative contribution factor $p_j(t)$ to the amplitude band SDNN(t).

The previously simulated frequency bands can be combined with the overall mean R-R trend as a function of time, yielding a more realistic representation of an R-R interval signal that integrates the influence of spectral components, as illustrated in Figure 4.

Accounting for residual variability

Real-world data invariably contain random noise that cannot be explained by further decomposing the signal into frequency bands without risking overfitting the inherent noise in R-R interval data. Nevertheless, the proposed model is capable of discerning the true signal from this noise, effectively isolating the underlying parameters that accurately reproduce both time and frequency components within a single generative framework.

An example of this signal-from-noise separation is depicted in Figure 5, where Gaussian random noise is added to highlight the true R-R interval components against the observed signal.

Making frequency bands change

To enhance the realism of our simulated R-R interval data, we introduce temporal variations in the proportional contribution of each frequency band to the overall signal amplitude. This dynamic approach moves beyond static assumptions of spectral composition, reflecting the inherent non-stationarity of physiological systems. To achieve this, we again leverage the flexibility of the double-logistic function, applying it to model the time-varying proportions of VLF, LF, and HF components.

We employ a stick-breaking scheme, a type of hierarchical decomposition, for the proportion components, denoted as $p_j(t_i)$. This elegant approach simplifies the modeling process significantly. Instead of defining and constraining three independent proportion parameters (p_{VLF}, p_{LF}, and p_{HF}), the stick-breaking method requires us to define only two latent variables. The first latent variable is the proportion of VLF (p_{VLF}) relative to the overall signal amplitude. The second is the HF proportion of the non-VLF remainder, which inherently encompasses both the HF and LF frequency bands. This structure naturally enforces the constraint that all proportions sum to unity at any given time point.

Initially, we model the proportion of VLF (p_{VLF}) using the same functional form as previously applied to RR(t) and SDNN(t), as defined in Equation 3 from the "Spectral Composition via Stick-Breaking" section. This consistency in functional form ensures parsimony and leverages the established interpretability of the double-logistic parameters. The remaining frequency parameters, specifically those for the HF and LF frequency bands, are then assumed to constitute the non-VLF portion of the signal. Conceptually, this can be expressed as $1 - p_{\text{VLF}} = p_{\text{HF}} + p_{\text{LF}}$. The following model parameter values were carefully selected to simulate realistic dynamics for $p_{\text{VLF}}(t)$:

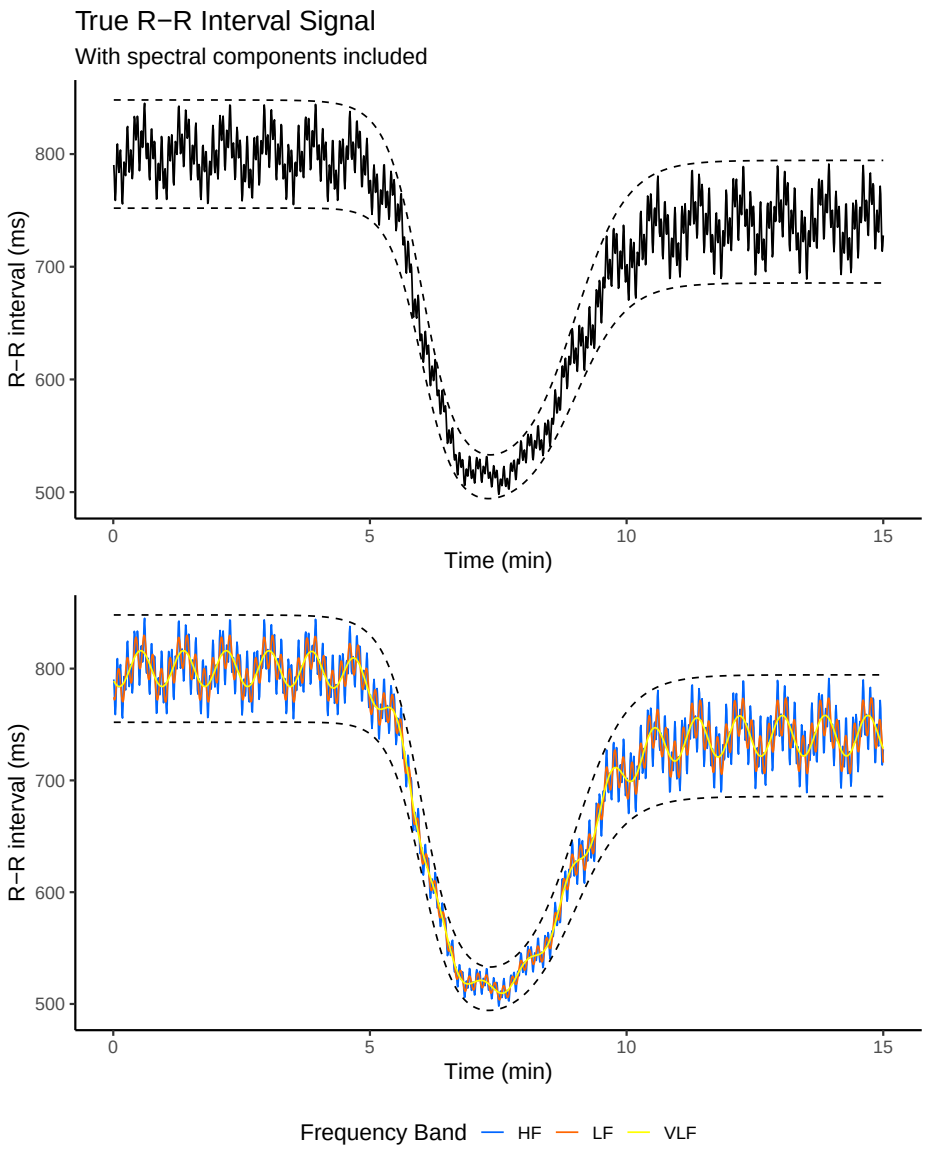

Figure 4: True generated R-R interval signal with time and frequency components integrated under the same generative process. The top panel displays the true signal, and the bottom panel highlights the frequency bands as part of the overall generated signal.

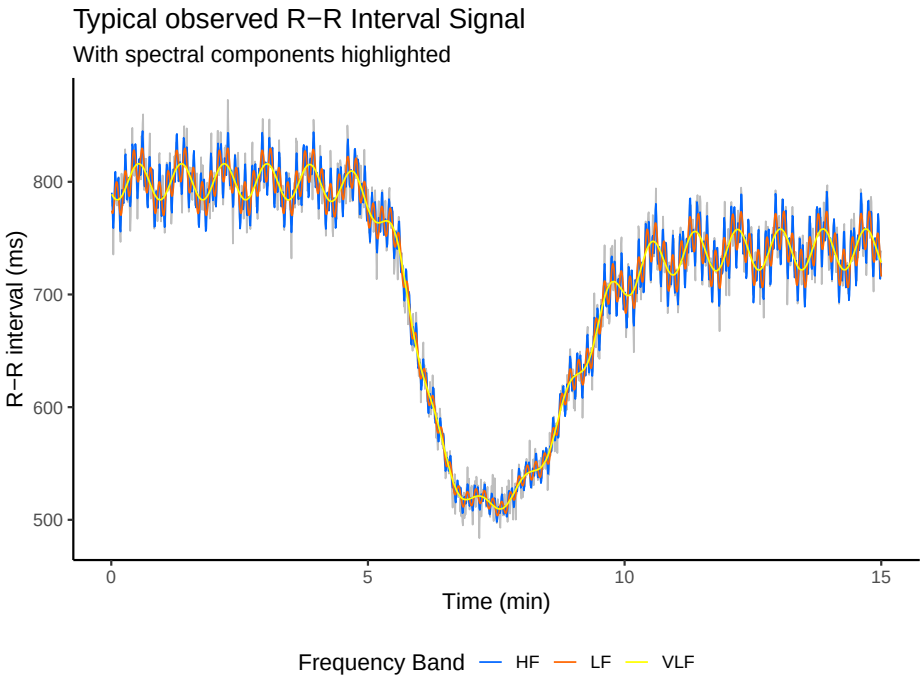

Figure 5: Generated R-R interval signal with Gaussian noise added, with true time and frequency components highlighted from the observed signal.

Parameter	Value	Meaning
α_{VLF}	0.15	Baseline proportion VLF
β_{VLF}	0.30	VLF proportion increase
c_{VLF}	1.00	Recovery proportion
λ_{VLF}	2.0	Drop rate
ϕ_{VLF}	1.0	Recovery rate
τ_{VLF}	6.0	Drop time
δ_{VLF}	3.0	Drop duration

These parameters dictate that the VLF contribution begins at a baseline of 15%, transiently increases by 30%, and fully recovers, with specified rates and timings. This reflects scenarios where VLF activity might be transiently accentuated or suppressed.

Subsequently, we model the ratio of HF to LF within the non-VLF remainder, denoted as $r_{\text{HF/LF}}(t)$, utilizing the functional form described in Equation 5 from the "Spectral Composition via Stick-Breaking" section. The parameters for this component are provided below:

Parameter	Value	Meaning
α_r	0.40	Baseline HF proportion
β_r	0.05	HF proportion decrease
c_r	0.5	Recovery proportion
λ_r	2.0	Drop rate
ϕ_r	1.0	Recovery rate
τ_r	6.0	Drop time
δ_r	6.0	Drop duration

These parameters indicate a baseline HF proportion (within the non-VLF part) of 40%, followed by a transient decrease of 5% and a partial recovery. The distinct recovery proportion ($c_r = 0.5$) highlights that the HF/LF balance might not fully revert to its initial state, reflecting a sustained shift in autonomic balance. The choice of $\delta_r = 6.0$ also suggests a longer duration for the recovery of this ratio compared to the VLF proportion.

By allowing the frequency bands to fluctuate dynamically within the constraints of this hierarchical decomposition, our model gains the capacity to represent a wider array of autonomic realities observable in experimental settings. Traditional spectral analyses often assume static band contributions, which can mask critical time-varying physiological responses. Our approach, by contrast, explicitly models these temporal shifts, offering a more nuanced and biologically faithful representation of heart rate variability. Furthermore, the ability to visualize the change in the proportional contribution of each frequency band over time, as illustrated in Figure 6, provides an intuitive understanding of these complex

dynamics. This visualization allows researchers to directly observe how the relative importance of sympathetic, parasympathetic, and very-low-frequency modulations evolves during a given physiological challenge or recovery period.

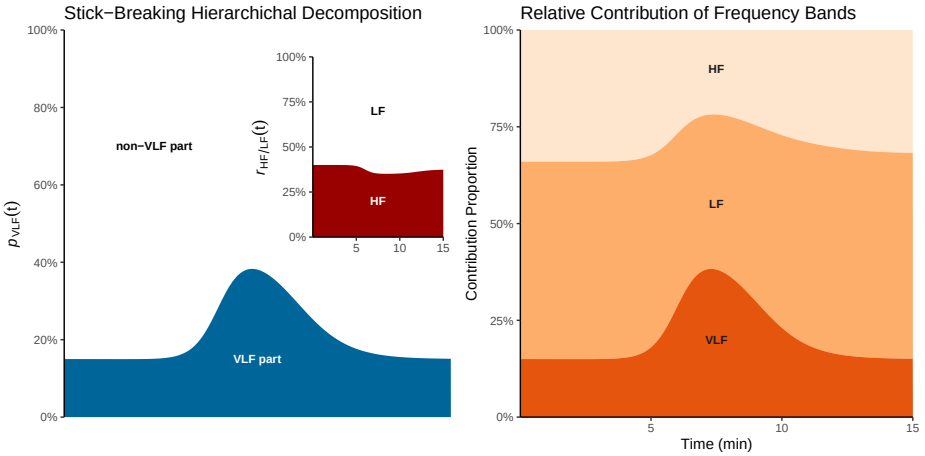

Figure 6: Stick-breaking strategy for hierarchical decomposition of temporal-dependent latent variables contributing to the relative contribution of each frequency band, isolating the frequency band components using hierarchical decomposition. In the top-left panel, we first model the VLF and non-VLF parts. In the top-right panel, we then use the non-VLF part to describe the change in the HF part of the non-VLF part. In the bottom panel, we observed the final composition of each proportion as part of the whole frequency band.

Now that we have successfully simulated time-varying frequency band contributions to the signal amplitude, the next crucial step is to integrate these dynamic spectral components into the overall observed R-R interval signal. This integration represents the culmination of our generative framework, allowing us to synthesize a realistic R-R signal that incorporates both non-stationary time-domain trends and fluctuating frequency-domain compositions. The resulting signal, depicted in Figure 7, is a comprehensive representation of a continuous R-R signal recording, effectively capturing the interplay of signal and inherent noise. This figure serves as a powerful demonstration of the model's ability to generate data that mirrors the complexity of real physiological measurements.

It is important to acknowledge that the subtle changes in the R-R signal stemming from the variations in the frequency bands may not be immediately apparent to the unaided eye in the overall R-R time series. These are often subtle modulations, embedded within the larger amplitude fluctuations governed by $\mathrm{RR}(t)$ and $\mathrm{SDNN}(t)$. However, their underlying presence is precisely what our model aims to capture and elucidate. This model represents a significant advancement, being among the first of its kind to accurately capture the intricate data generation process behind heart rate variability. Beyond merely simulating

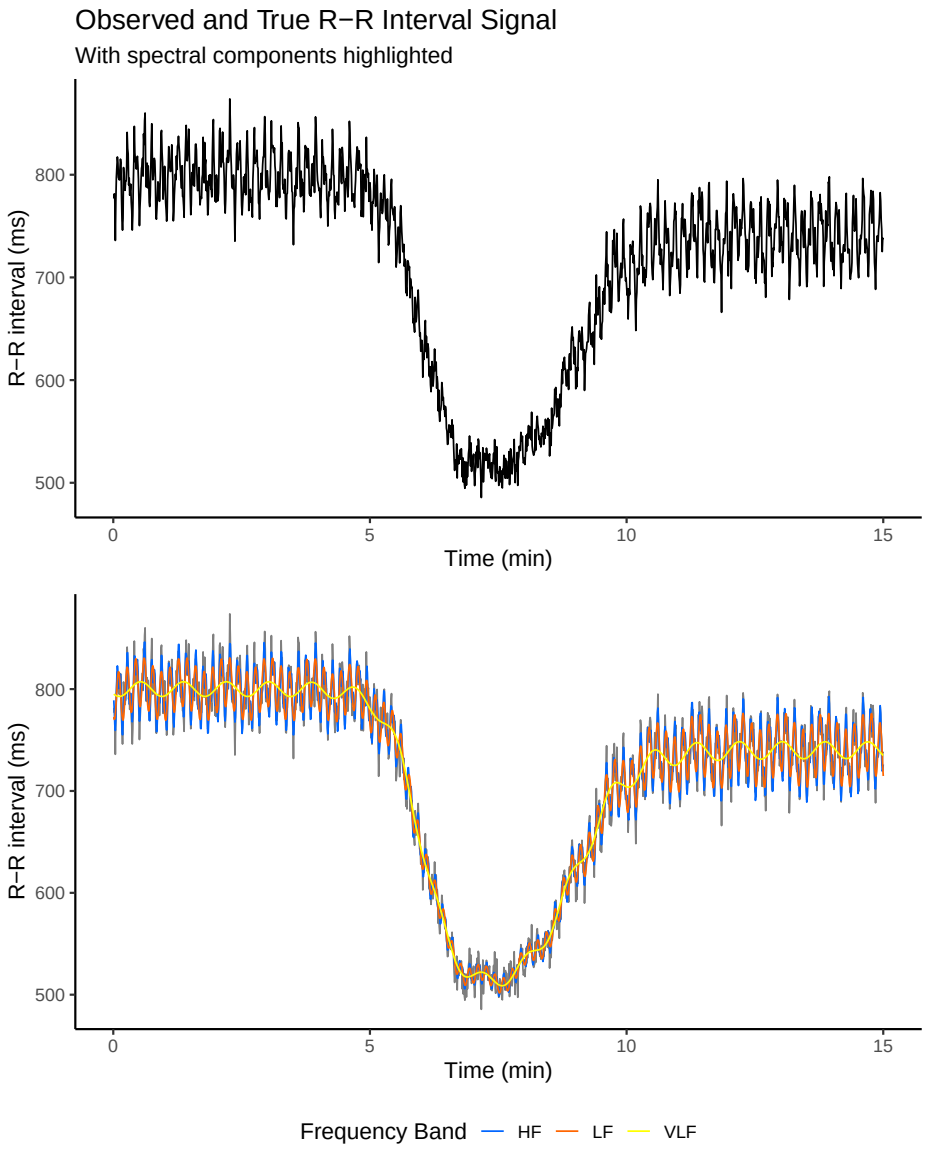

Figure 7: Observed and true R-R interval signal with time-varying spectral composition and band amplitudes, with frequency bands highlighted in the bottom panel.

data, this framework possesses the critical capability of estimating the temporal fluctuations of a real physiological signal by robustly mimicking its underlying spectral components. This dual capacity for both generation and estimation positions our model as a powerful tool for advancing the understanding of autonomic cardiovascular regulation in both health and disease.

Discussion

The generative model presented for R-R interval dynamics represents a substantial conceptual and methodological advancement in heart rate variability (HRV) analysis, explicitly addressing long-standing limitations within the field. Traditional approaches have consistently encountered an inherent compromise between temporal precision and frequency resolution in spectral techniques, alongside the predominantly descriptive nature of derived metrics that frequently obscure direct insight into underlying physiological mechanisms. Our novel parametric framework aims to transcend these limitations by providing a unified, time-varying representation of baseline heart period, overall variability amplitude, and spectral composition, thereby offering enhanced resolution, transparency, and clinical applicability. This integration into a single, comprehensive generative framework suggests a notable step towards overcoming these pervasive challenges.

A cornerstone of this model is its significant capacity to explicitly capture time-varying physiological processes. Unlike conventional fixed-window spectral analyses, which average activity over extended periods and thus inevitably blur transient autonomic events, our approach models each core component as a continuous function of time. The adoption of double-logistic functions for $\mathrm{RR}(t)$ and $\mathrm{SDNN}(t)$ allows for the precise characterization of dynamic changes, such as the onset and recovery kinetics observed during physiological challenges like exercise. This mathematical formulation enables the direct estimation of physiologically relevant indices, including surge onset times, peak amplitudes, and half-recovery durations, which are critical for understanding dynamic autonomic responses but are often obscured by aggregated metrics. For instance, the rapid vagal withdrawal or sympathetic surges occurring during orthostatic challenge or acute stressors, phenomena of substantial clinical relevance, may now be rigorously quantified without the analytical dilemma imposed by windowing techniques.

The model's innovative use of a two-stage stick-breaking decomposition for spectral proportions ($p_j(t)$) further distinguishes it from existing methodologies. This hierarchical approach intrinsically ensures that the proportional contributions of VLF, LF, and HF bands sum to unity at every time point, while simultaneously reducing the latent dimensionality of the system. By modeling the VLF proportion and then the HF-to-LF ratio within the remainder, the model accurately reflects an inherent biological hierarchy in autonomic control over heart rate variability. This contrasts with standard analytical practices that frequently reduce dynamic spectral information into aggregated, static in-

dices like the LF/HF ratio, which can ambiguously represent genuine increases in one component, decreases in another, or simultaneous modulations of both. Our model, by contrast, provides instantaneous, interpretable estimates of each band's dynamic contribution, offering a clearer perspective into the evolving balance of autonomic nervous system activity.

The physiological interpretability of the model's parameters is a considerable advantage. Each parameter within the double-logistic and stick-breaking formulations directly corresponds to a specific aspect of autonomic regulation, such as baseline levels, magnitudes of change, and rates of onset and recovery. This level of direct mechanistic significance, transitioning from descriptive to mechanistic insights, is often less explicit in other advanced HRV analysis techniques, such as nonlinear measures or data-driven decompositions. While methods like entropy or fractal dimension quantify signal complexity, they do not directly map to specific autonomic pathways. Similarly, many machine learning models, despite their predictive power, often operate as opaque "black boxes" devoid of readily apparent mechanistic interpretability. Our generative framework, by contrast, provides a transparent mapping from statistical parameters to physiological constructs, potentially facilitating clearer mechanistic inference and enhancing inter-study comparability.

A crucial implication of this unified generative paradigm is its ability to circumvent the time-frequency trade-off, a persistent methodological challenge in HRV analysis. By explicitly representing each latent component as a continuous, time-varying function, the model estimates instantaneous band-specific power without recourse to arbitrary smoothing or the use of sliding windows, which can temporally blur or obscure rapid sympathetic or parasympathetic modulations. This capability is achieved through the continuous, parametric representation of each component, supporting a high-resolution characterization of autonomic events. This approach may be particularly valuable for detecting abrupt physiological shifts that are often critical for diagnosis and intervention. The model's capacity to deliver precise, transparent, and mechanistically grounded insights into autonomic cardiovascular regulation represents a notable advancement in the field.

Furthermore, the generative nature of our model offers distinct capabilities beyond mere analysis. It can simulate synthetic RRI trajectories under controlled autonomic scenarios, a feature valuable for rigorous power analyses, hypothesis testing, and educational demonstrations. This simulation capability also allows for a deeper understanding of how time-varying frequency band contributions manifest in the overall RRI signal. While these spectral variations might be subtle and not immediately apparent to the unaided eye in a raw RRI time series, their underlying presence is precisely what the model is designed to capture and elucidate. This model represents a promising advancement, aiming to accurately capture the intricate data generation process behind heart rate variability.

Beyond simulation, the model possesses the capability of estimating the tempo-

ral fluctuations of a real physiological signal by robustly mimicking its underlying spectral components. This dual capacity for both generation and estimation positions our model as a potentially valuable tool for advancing the understanding of autonomic cardiovascular regulation in both health and disease. In basic research, it could facilitate mechanistic investigations into autonomic regulation, enabling quantitative assessment of coupling between respiratory patterns and heart rate, or precise delineation of recovery kinetics following physical exertion. Clinically, it may offer refined biomarkers for conditions such as dysautonomia, heart failure, and stress-related disorders, thereby potentially enhancing both diagnostic sensitivity and prognostic specificity. For wearable technology and biofeedback applications, the model could support real-time monitoring of autonomic state, which may guide adaptive interventions tailored to instantaneous physiological need. In essence, this formalized, physiologically coherent generative model of HRV aims to reconcile temporal and spectral analysis within a single, interpretable framework. By embedding parametric latent drives for baseline heart period, variability amplitude, and spectral composition, it is anticipated to contribute significantly to HRV research, fostering a transition from descriptive heuristics towards a quantitatively precise science of autonomic cardiovascular dynamics.

Limitations

Despite its significant advancements, the current generative model possesses certain limitations that warrant consideration. The primary limitation stems from its parametric nature, which relies on a predefined functional form for describing the temporal dynamics of baseline heart period, variability amplitude, and spectral proportions. While the double-logistic function offers considerable flexibility and physiological interpretability, it may not universally capture all conceivable patterns of autonomic modulation, particularly those exhibiting highly irregular or non-monotonic behavior not well approximated by sigmoidal curves. The model also assumes a fixed number of frequency bands and their approximate central frequencies, which might not account for individual variability in spectral composition or shifts in resonant frequencies under extreme physiological states. Furthermore, the current implementation does not explicitly model or differentiate between the precise neural pathways contributing to each frequency band, relying instead on the established physiological interpretation of VLF, LF, and HF components. The generalizability of the proposed parameterization may also be influenced by the specific population and experimental conditions under which the model is applied and validated.

Future Research

Future research endeavors will focus on expanding the model's capabilities to address its current limitations and unlock further insights into autonomic regulation. One key direction involves exploring more flexible, non-parametric or semi-parametric extensions to the functional forms, allowing for a broader

range of temporal dynamics to be accurately captured without sacrificing interpretability where possible. This could include incorporating basis functions or Gaussian processes to model more complex RRI trajectories and spectral shifts. Investigations into data-driven approaches for identifying optimal frequency band definitions and their potential time-varying characteristics are also warranted, moving beyond fixed ranges to account for individual physiological differences. Integrating biophysically detailed models of neural autonomic control into the generative framework represents another promising avenue, which could allow for the explicit modeling of efferent and afferent sympathetic and parasympathetic pathways, thereby providing a more granular understanding of the physiological origins of HRV. Furthermore, rigorous validation across diverse clinical populations and a wider array of physiological challenges is crucial to establish the model's robustness and clinical utility. Comparative studies against state-of-the-art non-linear and machine learning approaches will also be essential to quantitatively demonstrate the enhanced insights provided by our mechanistic, interpretable framework. Ultimately, the development of software tools facilitating the broad adoption and application of this generative model will be paramount for its integration into mainstream HRV research and clinical practice.